Laser-induced crystallization of amorphous GeTe: A time-resolved study

E. Huber and E. E. Marinero
IBM Almaden Research Center (K67/802), San Jose, California 95120
(Received 30 January 1987)

Amorphous thin films of GeTe were exposed to excimer-laser pulses of fluences between 3 and 27 mJ/cm^2. Transient reflectivity and conductivity were simultaneously recorded during the laser interaction with a time resolution of a few nanoseconds. A rapid increase in R and σ due to laser-induced heating is observed. This is followed by a decrease of these parameters at a slower rate due to cooldown. During the cooldown process and within a certain temperature interval nucleation and growth are possible and experimentally observed. The cooling rate in this interval is a function of incident fluence and determines the degree of crystallization induced by laser irradiation. Above a fluence of 22 mJ/cm^2 the films crystallize to a large degree within 200 ns (25% and greater than 90% at 23 and 27 mJ/cm^2, respectively). Between 15 and 22 mJ/cm^2 the crystallization is less than a few percent (frustrated crystallization), and application of a subsequent pulse leads to an extremely fast crystallization (50 ns). Below 15 mJ/cm^2 the irradiated films remain amorphous. A model describing transient R and σ in terms of cooling, nucleation, and growth is presented and compared with the measured transient profiles.

I. INTRODUCTION

GeTe and ternary alloys based on GeTe are currently of interest for reversible optical storage due to their structure-dependent optical properties.[1] *Amorphous* GeTe is a semiconductor with a band gap of 0.8 eV and a low electrical conductivity σ at room temperature [10^{-3} $(\Omega\,\mathrm{cm})^{-1}$, see Bahl and Chopra[2]]. As typical for semiconductors, the temperature coefficient of resistivity (TCR) is negative.[2] The room-temperature reflectivity R at 633 nm is 40% (our measurements; see also Fisher and Spicer[3]). The *liquid* state, although structurally related to the amorphous state, has an electrical conductivity of about $(2-3)\times10^3$ $(\Omega\,\mathrm{cm})^{-1}$ at the melting point (see Tschirner *et al.*,[4] Valiant and Faber,[5] or Glazov[6]), with increasing metallic character at higher temperatures. Near the melting point (1000 K), the TCR is approximately -0.7 $\mu\Omega$ cm/K (Refs. 4 and 7) consistent with the Mooij correlation[8] which states that the TCR is negative for disordered metallic phases with resistivities exceeding 150 $\mu\Omega$ cm [$\sigma<6000$ $(\Omega\,\mathrm{cm})^{-1}$]. For higher temperatures (above 1200 K), the TCR of liquid GeTe increases to zero (or even to a small positive value).[7] The reflectivity at 633 nm is estimated to be 50–60% based on data for liquid Te (Ref. 9) (47%) and liquid Ge (Refs. 10 and 11) (65–70%). *Crystalline* GeTe is a semiconductor with a very small band gap (0.1 eV) and an almost metallic conductivity of 3×10^3 $(\Omega\,\mathrm{cm})^{-1}$ at room temperature [our measurements on oven-crystallized films and literature values[2,12] range $(3-5)\times10^3$ $(\Omega\,\mathrm{cm})^{-1}$]. The TCR at room temperature is positive,[2,12] which is typical for metals. The reflectivity at 633 nm is 65% (our measurements on oven-crystallized films; see also Fisher and Spicer[3]).

The amorphous and the crystalline states of GeTe can be easily distinguished by reflectivity, R, and conductivity, σ, measurements. *Time-resolved* measurements of laser-irradiated chalcogenide semiconductors offer an opportunity to study the transformation kinetics between different phases[13,14] in real time. In this paper we report studies on crystallization of amorphous GeTe thin films (200 nm) induced by excimer-laser irradiation. Of particular interest is the degree of crystallization obtained as a function of laser fluence. In contrast to amorphous Si, no first-order phase transition is involved in the transformation from the liquid to the amorphous GeTe state. Thus, concepts such as melt velocity and melt front, which are appropriate for amorphous Si laser studies[15,16] are *not* suitable for amorphous GeTe. Rather, we must consider a smooth (although steep) change from "glassy" to "liquid" ordering with a smooth change of the electronic properties. This distinction has an important consequence for the fluence dependence of the transient R and σ profiles. Generally speaking, crystalline films show a distinct threshold behavior at high fluences, indicating the discontinuous change from the crystalline to the liquid state, while the amorphous films undergo a smoother change at lower fluences.

The purpose of this paper is to study the transient changes of the electronic properties of amorphous GeTe films irradiated with 12-ns laser pulses. From these measurements, cooling and crystallization rates may be obtained. These quantities are—among others—the limiting factors for high-speed read and write optical memory application.

II. EXPERIMENTAL PROCEDURE

Amorphous thin films of GeTe were prepared by vapor deposition onto glass substrates (for x-ray measurement we also used sapphire substrates) in a vacuum better than 10^{-6} mbar.[13,14] The GeTe layer was deposited with a thickness of 200 nm and in the shape of

elongated stripes (1 mm×5 mm) with Al contacts on both sides. Figure 1 shows the experimental setup used for the transient reflectivity and conductivity measurements. The annealing laser is a KrF excimer laser (248 nm), providing 12-ns pulses with fluences up to 70 mJ/cm^2. In this experiment the incident laser fluence is varied by a variable attenuator and is monitored by a pyroelectric detector and a storage oscilloscope. A constant bias voltage (10 V) is applied to the sample using a specially designed solid Cu sample holder. The current is a function of the resistance of the sample and is measured as a voltage drop across the 50-Ω input resistor of a 500-MHz bandwidth transient digitizer.[14] The measured voltage U is related to the (overall) conductivity of the film by the following equation (for a full description of the technique and the derivation of the conductivity values see Pamler and Marinero[14] and Thompson *et al.*[17])

$$\sigma = \frac{1000}{\frac{2}{U} - 0.4} , \tag{1}$$

where σ and U are in $(\Omega\,\mathrm{cm})^{-1}$ and V, respectively. Since the measurement is not a four-point measurement, contact resistance must be taken into account. The contact resistance was estimated to be 10 Ω and corrections were included; however, typical resistances measured in this work exceed 200 Ω and thus one can neglect contact resistivities. The Ohmic character of the contacts was guaranteed using a sufficiently high bias voltage (10 V). The reflectivity was measured using a He-Ne laser in combination with a fast photodiode and a storage oscilloscope. The signal on the scope is directly proportional to the reflectivity of the sample in percent (in our case 19 mV per %). The photodiode signal was filtered with a narrow-band notch filter to suppress the 500-MHz modulation produced by mode competition in the He-Ne laser. A second fast photodiode is placed near the exit window of the excimer laser to detect stray light in order to provide a trigger signal for the digitizer and the scope. The irradiated area was chosen to be slightly larger than the sample size and all the experiments were *single-shot* measurements. The absolute errors of reflectivity and fluence are estimated to be 2% and 1 mJ/cm^2, and the relative error of conductivity to be 10%.

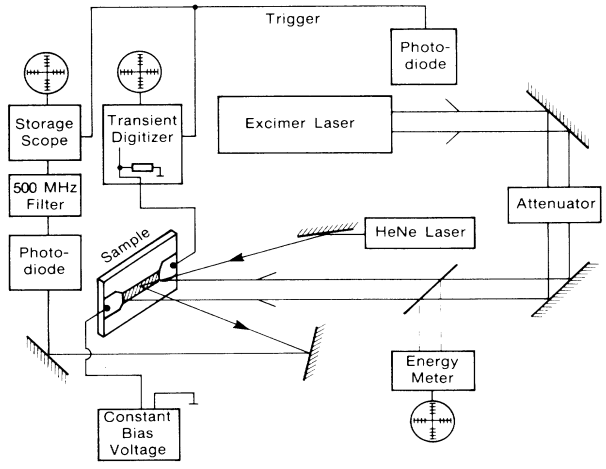

FIG. 1. Experimental setup for simultaneous time-resolved optical and electrical studies in GeTe thin films.

In addition, optical and electron microscopy and x-ray analysis of the laser-irradiated films were also performed, as well as measurements of the overall changes in R and σ following the laser exposure (equilibrium values).

III. RESULTS AND DISCUSSION

Time-resolved reflectivity and conductivity profiles for fluences of 17 and 22 mJ/cm^2 are shown in Fig. 2 [the conductivity is given as a voltage signal U according to Eq. (1)]. The complex transient profiles observed mirror the physical transformations induced. As indicated in Fig. 2, the evolution of the transformation occurs after the termination of the annealing laser pulse. The shapes of the transient profiles strongly depend on the incident fluence and may be grouped into four fluence regimes. These regimes are as follows: (1) below 5 mJ/cm^2 (very low fluence); (2) 5–15 mJ/cm^2 (low fluence); (3) 15–22 mJ/cm^2 (intermediate fluence); and (4) above 22 mJ/cm^2 (high fluence). Permanent changes of R and σ are small in regimes (1)–(3) and large in regime (4); the ablation limit is 26 mJ/cm^2. Figure 3 summarizes this behavior, showing the most salient features. The values given on the vertical axes are typical for the corresponding regimes.

As shown in Fig. 3, at very low fluences (*regime 1*), a slight reflectivity increase (a few tenths of a percent) can be seen, which is proportional to the fluence. The conductivity change is below our detection limit [2 $(\Omega\,\mathrm{cm})^{-1}$]. Photogeneration of carriers and/or simple heating may account for the reflectivity increase. No major modification of the material occurs in this regime and it thus will not be of main interest in this work.

In *regime 2* (5–15 mJ/cm^2) a large reflectivity peak on top of the small feature mentioned in regime 1 can be observed. A similar peak appears in conductivity. This behavior indicates that the films undergo major structural and electronic modifications ("melting," see Sec. I). For both the conductivity and the reflectivity, the magnitude of the peak first increases linearly with the fluence. The

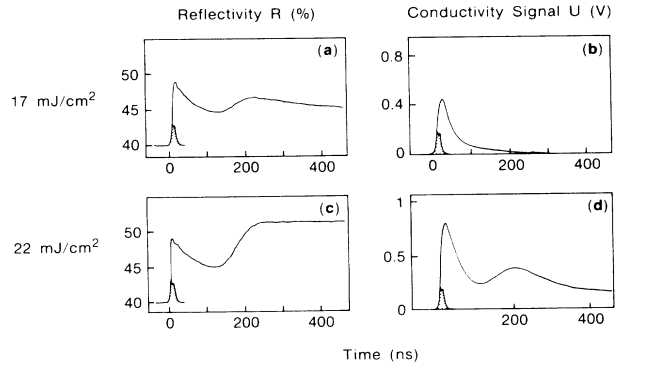

FIG. 2. Typical transient reflectivity and conductivity profiles of GeTe thin films for fluences of 17 [(a) and (b)] and 22 mJ/cm^2 [(c) and (d)]. For comparison, the temporal development of the laser pulse is included.

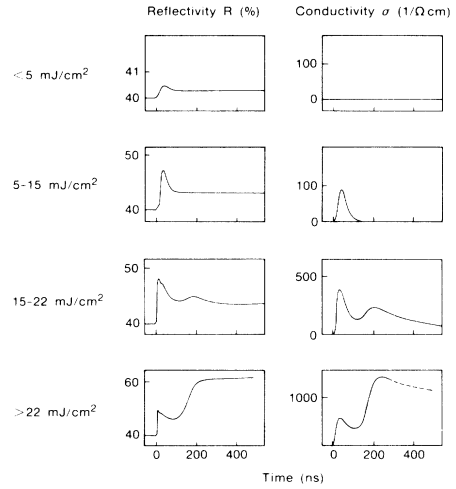

FIG. 3. Fluence dependence of reflectivity and conductivity profiles of GeTe thin films. Typical profiles for the fluence regimes 1–4, as described in the text, are given.

reflectivity peak begins to saturate at around 8 mJ/cm^2 and attains a constant value of 50% above 12 mJ/cm^2. On the other hand, the conductivity peak only appears to saturate for fluences near the ablation limit (26 mJ/cm^2). This obvious difference demonstrates that above 8 mJ/cm^2 the laser-induced structural modification has reached the skin depth of He-Ne light [estimated to be 20–30 nm (Ref. 18)]. With increasing laser fluence the modification goes deeper into the material as shown by the further increase in conductivity, while these changes are no longer detected optically. It is noted that even near the ablation point (26 mJ/cm^2) the peak conductivity immediately following laser irradiation is approximately a factor of 4 times lower than that expected for a fully molten film. Since the conductivity of liquid GeTe increases with temperature (negative TCR, see Sec. I), this effect cannot be accounted for by overheating of the liquid above the melting temperature. We thus infer that the laser-heated volume does not attain the properties of a fully liquified structure. We also mention that small permanent reflectivity changes (3% or less) occur in regimes 1 and 2. These changes might be caused by surface modifications and/or structure relaxation (i.e., reaching of another amorphous configuration) induced by short laser irradiation.

In *regime 3* (15–22 mJ/cm^2) a broad second peak appears on the falling (cooling) edge of both the conductivity and the reflectivity profile. The appearance in time increases with fluence from 80 to 120 ns, indicating that the process associated with this peak is temperature initiated. This new structure in the profile (second peak) is interpreted in terms of nucleation and growth of the crystalline phase as follows.

The temporal development of the first peak indicates the point at which the material has reached its maximum overall temperature. The falling edge marks the subsequent cooldown of the film. The nucleation and growth rates of crystallites[19] have a maximum at a certain temperature T_n: it is zero both at very high (thermodynamic limit) and at very low temperatures (kinetic limit).[20] Fast crystallization is possible in a temperature interval γ around T_n.[21–23] The degree of crystallization reached during the cooldown process depends on the time t_γ during which the film temperature is between $T-\gamma/2$ and $T+\gamma/2$. If the cooling rate in this temperature interval is too high, no crystalline material is formed. If it is too low, complete crystallization may occur. In laser annealing, the cooling rate at a *fixed* temperature decreases with fluence.[24] Thus, at intermediate fluences the cooling rate at T_n can allow a small degree of crystallization which results in a small increment in R and σ about 100 ns after the temperature maximum. This gives rise to the second broad peak evident in Fig. 3.

A few differences in the appearance of the second transient peak may be noted for the conductivity as compared to the reflectivity profiles (see Figs. 2 and 3). In the former profiles, the peak is more pronounced and develops at relatively higher fluences. It is still present at fluences for which the change in reflectivity has become permanent. This is again explained by the fact that reflectivity monitors only processes in the skin depth. Further, the conductivity of a material containing conducting crystallites embedded in an isolating matrix is governed by the percolation process[25] which shows threshold behavior at a critical volume fraction of conducting crystallites (percolation threshold). This will be further discussed in Sec. IV.

Evidence for frustrated crystallization is provided in Fig. 4 in which we present transient reflectivity changes ΔR obtained when two subsequent pulses of the same fluences are applied onto the same spot [4(a) first pulse; 4(b) second pulse]. For low fluence the first and second profiles are almost identical. For intermediate fluences the crystallization process initiated by the second pulse is accelerated by the presence of small crystallite nuclei formed after the first pulse. This implies that the laser-heated volume does not liquify completely. Thus, extremely fast crystallization is observed while the laser still delivers energy to the samples, and is complete within 50 ns following the maximum temperature rise. For high

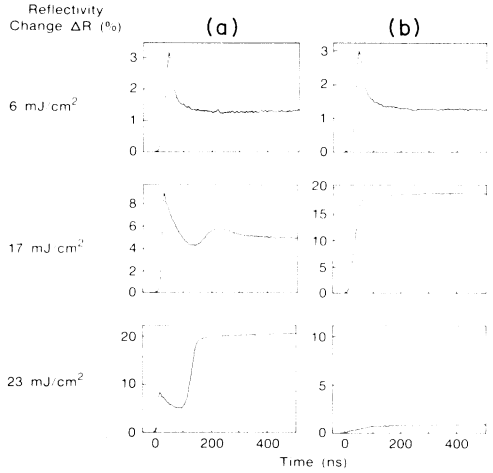

FIG. 4. Reflectivity changes of GeTe thin films at various fluences induced by (a) a single pulse and (b) a subsequent pulse of the same fluence.

fluences complete crystallization (at least throughout the skin depth at 633 nm) has occurred after the first pulse and the second pulse has no influence. For very high fluences of the second pulse (above 35 mJ/cm^2) melting of the crystallized film is observed.

Since this regime appears to be the most interesting regime for the crystallization kinetics of GeTe, reflectivity measurements were also performed on *nonstoichiometric* films (45 and 55 at. % Ge). Long-range atomic diffusion is required for crystallization and we expect the crystallization process to slow down. This is, in fact, observed for the Te-rich films: the transient profiles obtained after a few subsequent laser pulses are similar to each other and all show the characteristic second peak. This demonstrates that only a small degree of crystallization is accomplished by each single pulse. After a sufficient number of pulses complete crystallization can be obtained. For Ge-rich films, the second peak, characteristic for frustrated crystallization, is also observed,[26] however, the crystallization process induced by the second pulse is as fast as for stoichiometric films and complete crystallization [at least throughout the skin depth at 633 nm] is readily obtained. We thus infer that excess of Ge does not decrease the crystallization velocity and that partitionless crystallization may still be possible. We also note that between 45 and 55 at. % Ge the viscosity decreases with Ge content, as opposed to many other Te alloys, for which the liquid assumes maximum viscosity at the composition of the corresponding compound.[27]

Corroboration that the optical and electrical changes observed during laser annealing are due to crystallization of amorphous GeTe is given by x-ray diffraction studies of comparable samples ($Ge_{55}Te_{45}$ on sapphire) that are subjected to the fluence regimes previously discussed. In Fig. 5, x-ray analysis of an as-deposited sample [Fig. 5(a)] is compared to laser-exposed films [Figs. 5(b) and 5(c)] as well as to a fully crystallized film, obtained by oven heating of an amorphous sample to 520 K for 1 h [Fig. 5(d)]. Only the characteristic sample background is evident in 5(a) whereas in the case of 5(c) and 5(d) prominent diffraction peaks corresponding to crystalline GeTe can be seen. Following laser exposure of 15 mJ/cm^2 (Ref. 26) only traces of these peaks are apparent in Fig. 5(b). This indicates that both the number density and the size of the crystallites generated in this fluence regime are small. We estimate that for this fluence, based on the resolution of the x-ray diffractometer, the crystalline size is between 100 and 200 Å (or, if the grains are larger, there are very few of them, less than 5% of the film). We note that in the regime of frustrated crystallization the size of the generated crystallites depends on fluence, film composition, and substrate material. However, significant nucleation occurs as a consequence of this single-pulse irradiation and thus, when the same area is exposed to a subsequent pulse, rapid crystallization takes place, as evident in Fig. 5(c). It is apparent that the diffraction patterns for the laser-annealed 5(c) and oven-annealed samples 5(d) show differences. A preliminary analysis of the phases indicates that during laser annealing a slightly distorted rhombohedral structure is obtained, whereas oven annealing leads to an orthorhombic phase (or mixture of phases).

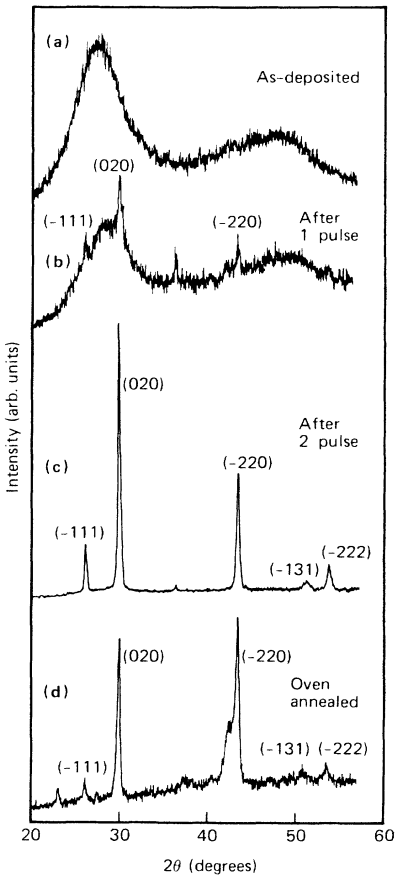

FIG. 5. X-ray analysis of $Ge_{55}Te_{45}$ thin films as deposited on sapphire (a), exposed to (b) one and (c) two pulses of 15 mJ/cm^2 (see Ref. 26). In (d) the diffraction pattern of an oven-annealed sample is shown for comparison.

This will be further investigated.

Additional evidence for frustrated crystallization is provided by transmission electron microscopy (TEM) analysis of samples ($Ge_{55}Te_{45}$ on glass) exposed to single and to two consecutive laser pulses. To this aim, the glass substrate was first chemically etched and then ion milled to yield specimen thicknesses suitable for plan-view TEM analysis. Figure 6(a) shows an area within the region exposed to a single laser pulse of 13.5 mJ/cm^2.[26] Substantial nucleation and growth have taken place within the amorphous matrix (other areas within the exposed region show different grain sizes due to inhomogeneous irradiation). It is noted that selected area diffraction (SAD) analysis of the as-deposited sample reveals only an amorphous structure, at least within the resolution of the instrument (30 Å). The polycrystalline grains in Fig. 6(a) exceed 400 nm (film thickness of 200 nm), indicative that the kinetics of crystallization in this material is extremely rapid to permit substantial growth during the cooldown. In Fig. 6(b), the image of an area irradiated with two subsequent pulses of the same fluence is shown. Full crystallization is induced by the second pulse and the SAD pattern corresponds to crystalline GeTe. No remnant

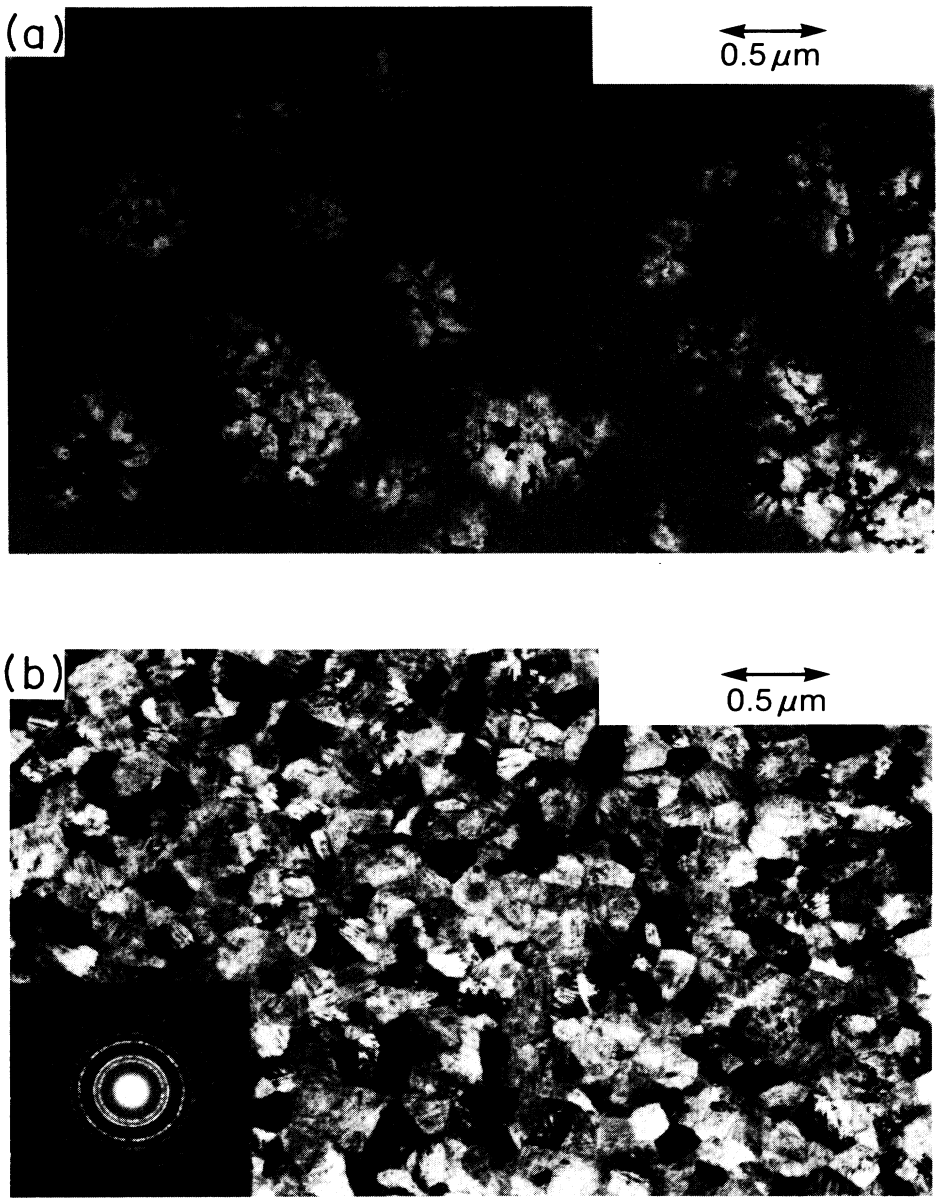

FIG. 6. TEM analysis of $Ge_{55}Te_{45}$ thin films exposed to (a) one and (b) two pulses of 13.5 mJ/cm^2 (see Ref. 26). Significant grain growth is observed in (a) whereas (b) shows complete crystallization of the irradiated area.

amorphous material can be observed and the grain size is large (1000 Å). We thus infer that the first laser pulse leads to significant nucleation and, depending on fluence, to grain growth. The nuclei are small and are probably distributed within the laser-excited volume that exceeded the temperature T_n for a critical time period (see Sec. IV). Applying a second pulse of the same fluence, leads to extremely fast growth of the seeded area resulting in the optical and electrical changes reported in this work.

The small shoulder which develops after the main peak of the transient reflectivity profile of GeTe [see Figs. 2(a) and 2(c)] appears to be correlated to the crystallization process, since it can be seen only in regimes 3 and 4. For the Te-rich films which crystallize after repeated irradiations, the shoulder can be seen after every pulse. For Ge-rich films this shoulder is very small. The origin of this small structure is not clear. We might speculate that it marks the formation of nonstoichiometric crystallites in the presence of excess of Te.[28] We also note that a similar shoulder is reported for the surface temperature of Si, as calculated by Baeri and Campisano.[29] The observation that the shoulder does not appear in the conductivity may be explained by the fact that the process resulting in the shoulder either remains below the percolation threshold or is a mere surface effect.

Finally, in *regime 4* (>22 mJ/cm^2) the second peak in

the transient profiles does not decay in time: large permanent changes in reflectivity and conductivity occur after about 200 ns. This is shown in Fig. 7. In the case of R, equilibrium values (taken at $t > 1$ μs) are given; these values are about 2% larger than the transient values obtained after 200 ns (end of crystallization) due to the negative temperature coefficient of reflectivity (see Baleva[18]). In the case of σ, the equilibrium and the transient values (taken at $t = 200$ ns) are given. The equilibrium values are about a factor of 4 smaller due to stress cracks (see below). Literature data as well as our own measurements of oven-crystallized films are also included for comparison. Above 23 mJ/cm^2 for R and 27 mJ/cm^2 for σ, the values obtained are comparable to those for crystalline GeTe. We thus infer from Fig. 7 that films irradiated with fluences of 23 and 27 mJ/cm^2 have crystallized to a degree of approximately 25% and $>90\%$, respectively. The onset of reflectivity changes occurs at lower fluences than for conductivity. This is due to the fact that reflectivity is surface sensitive whereas conductivity must also obey percolation laws. Permanent changes of conductivity are not observed below a fluence of 23 mJ/cm^2. This demonstrates the dependence of conductivity to formation of interconnecting crystallites at the percolation threshold. The apparent discrepancy, as mentioned above, between the permanent conductivity and that obtained after 200 ns arises from the following reason: we have observed that above 23 mJ/cm^2 stress cracks develop in the material. These cracks are probably caused by the 7% volume change upon crystallization[30] and the thermal stress induced by the rapid cooldown after the laser pulse. Since cracking is not observed upon irradiation of very thin amorphous (75 nm) as well as of 200-nm oven-crystallized samples at comparable and higher fluences,

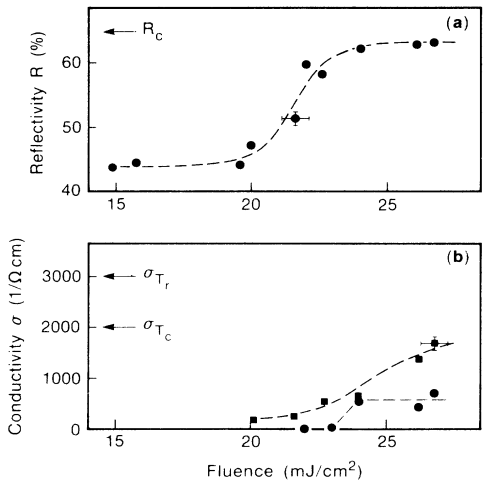

FIG. 7. (a) Reflectivity and (b) conductivity changes of single-laser-exposed GeTe thin films as a function of fluence (●, equilibrium values, taken at $t > 1$ μs; ■, transient values, taken at $t = 200$ ns). Data for polycrystalline GeTe from the literature and from our measurements (see Sec. I) are included for comparison: R_c, σ_{T_c}, σ_{T_r} refer to reflectivity, conductivity at 460 K (crystallization temperature), and conductivity at room temperature, respectively.

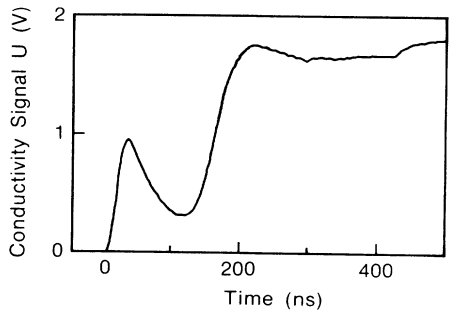

FIG. 8. Transient conductivity profile of a GeTe thin film for a fluence of 26 mJ/cm^2. Note the irregular pattern at 300 and 400 ns. Microscope examination revealed stress cracking following laser exposure.

we infer that an unmolten amorphous layer at the bottom of the film is required for cracking. Figure 8, which illustrates the transient conductivity obtained for a case that led to stress cracking, indicates that the onset of cracking is not driven by temperature but rather by crystalline growth. We infer that the onset of cracking occurs approximately 300 ns after the temperature maximum—as evidenced by discontinuous and nonreproducible conductivity changes.

In the next section we present a model for the experimentally measured transient conductivity and reflectivity profiles based on simple thermodynamic and kinetic assumptions. We will show that all the experimental profiles can be reproduced by the model in a consistent manner.

IV. MODELING OF THE REFLECTIVITY AND CONDUCTIVITY

The irradiated amorphous film is rapidly heated up during the pulse and cools down at a slower rate after the pulse. However, no first-order phase transition is involved and there is never a real melt front but only a "hot" amorphous material. The film can be more glasslike or more liquidlike depending on temperature. The peak temperature T_{max} is a function of the incident laser fluence f and the thermodynamic properties of the amorphous film. A calibration of $T_{max}(f)$ is obtained using results for crystalline GeTe films exposed to laser pulses.[14] For such films, the fluence at which the surface begins to melt was determined to be 23 mJ/cm^2 (approximately 35 mJ/cm^2 for melting throughout the skin depth). Taking the lower thermal conductivity of the amorphous material[31,32] into account, the threshold for reaching the melting temperature (1000 K) may be expected at 15–20 mJ/cm^2. These values belong to regime 3 and are thus consistent with the observation that crystallization occurs in this regime.

Laser irradiation-induced crystallization is described by a time-dependent crystalline volume fraction $v_c(t)$. Disregarding the fact that both T and v_c have a *distribution* in thickness we use overall values for the whole film [temperature variations in thickness are shown to be less than 20 K after a few ns (Ref. 24)]. The thermodynamic part of the model is based on two assumptions.

First assumption: the sample (film + substrate) is a homogeneous infinite solid and linear heat flow takes place. Since the thermal diffusivity κ of the GeTe film, as calculated from the thermal conductivity and the specific heat, is larger than (or at least equal to) that of the glass substrate used [0.005 cm^2/s (Ref. 33)], the cooldown rate is mainly determined by the substrate and we neglect the influence of the film. Analytical solutions for the time dependence of the temperature $T(t)$ are given by Baeri and Campisano[29] and Carslaw and Jaeger.[34] For $t > 20$ ns, where the condition $\sqrt{\kappa t}$ is greater than the film thickness is satisfied and $T(t)$ is reduced to (all temperatures in K)

$$T(t)=300+(T_{\max}-300+\Delta T)\frac{d}{\sqrt{\pi\kappa t}} , \tag{2}$$

where $T_{\max}$, the maximum temperature of the film, is a *parameter* that depends on the incident laser fluence,[35] κ is the thermal diffusivity of the glass substrate, and d is the film thickness. The correction term ΔT accounts for the latent heat of crystallization. The use of a correction term ΔT (for ease of computation ΔT is considered as a small perturbation) added to the temperature $T(t)$ is a rough approximation. For a more detailed analysis see Carslaw and Jaeger.[36] ΔT is assumed to be zero before the onset of crystallization (no latent heat produced) and then to increase linearly with time. After the end of crystallization ΔT is assumed to remain constant at the value $v_{\text{tot}}\Delta H_c/c_p$, where v_{tot} is the total volume fraction of crystalline material produced during the crystallization process, ΔH_c is the heat of crystallization from the glass [heat of "devitrification," 20 cal/g (Ref. 37)], and c_p is the specific heat of glassy GeTe [approximately 0.1 cal/g K (Ref. 38)]. With these values $v_{\text{tot}}\Delta H_c/c_p$ becomes $v_{\text{tot}}\times 200$ K. In order to simplify the calculation, v_{tot}, the total volume fraction of crystalline material produced upon irradiation, is approximated by νt_γ, where t_γ is the time interval during which the crystallization process actually occurs (see Sec. III), and ν is the nucleation and growth frequency[19] [see Eq. (3)].

Second assumption: the rate of crystallization as a function of temperature is assumed to be a Gaussian curve (peak at T_n and width γ, see Sec. III). Above $T_n+\gamma/2$ it is too hot (thermodynamic limit, small driving force) and below $T_n-\gamma/2$ it is too cold for crystallization (kinetic limit, slow kinetics). At T_n optimum conditions allow fast crystallization. We note that the nucleation rate in a supercooled liquid, as well as the crystalline growth velocity, have bell-shaped temperature dependences.[39] Thus, as a phenomenological approach, we write for the increase of volume fraction of crystalline material as a function of temperature T

$$\dot{v}_c(T)=\nu\exp\left[-\left[\frac{T-T_n}{\gamma/2}\right]^2\right] . \tag{3}$$

The nucleation and growth frequency[19] $\nu=VI$, where I is the specific frequency (in $cm^{-3}s^{-1}$) and V is the volume of the sample (10^{-6} cm^3), enters as an adjustable *parameter*. The time needed for complete crystallization at the temperature T_n is $1/\nu$. Using the equations given by Turnbull[39] the nucleation rate for GeTe assumes its maximum value at a reduced temperature (the temperature divided by the melting temperature) of approximately 0.65 corresponding to $T_n=650$ K. For γ, an upper limit of approximately 150 K is given by the fact that below the glass temperature T_g the crystallization rate must be zero and we thus choose $\gamma=100$ K. If the temperature T varies with time the volume fraction $v_c(t)$ as a function of time is given by

$$v_c(t)=\int_0^t \dot{v}_c(T(t'))dt' , \tag{4}$$

where $T(t')$ is defined by Eq. (2). $v_c(t)$ increases, of course, with time and it may reach the value 1 (film has completely crystallized) if the film temperature remains at T_n sufficiently long. Values for v_c larger than 1 are not reasonable and the integral is clipped at that value. The time dependences of T and v_c [Eqs. (2) and (4)] define the thermodynamic and structural state of the material in time on the basis of two parameters: $T_{\max}$, the maximum temperature of the film, and ν, the nucleation and growth frequency.[19]

We must now connect v_c with the measured quantities R and σ. For the reflectivity R as a function of v_c, the volume fraction of crystalline material, we choose the following intuitive approach: R is assumed to change from the amorphous to the crystalline value obeying a smooth step function. This takes into account that the reflectivity assumes the crystalline value when a planar crystallization has occurred throughout the skin depth but not necessarily throughout the whole film. We thus write

$$R=(0.65-R_a)\frac{v_c^4}{v_c^4+\alpha^4}+R_a , \tag{5}$$

where R_a and 65% are the reflectivities of the hot amorphous and the crystalline material, respectively. Since the main contribution to the temperature dependence of R in our films arises from the temperature dependence of the amorphous material and from the degree of crystallization, we neglect the small temperature coefficient of the crystalline reflectivity [from the slope of $R(t)$ after crystallization we estimate -0.01% per K; see also Baleva[18]]. The shape parameter α was chosen to be 0.5. Equation (5) could be further improved by using the actual thickness distribution of v_c and the effective medium theory (EMT).[40] However, since the thickness distribution of v_c is not known and knowledge of the complex dielectric function is required for EMT, we use (5) as a simple numerical approximation to a complex phenomenon.

As mentioned before, in the case of the conductivity we have to take percolation[25] into account: below a certain threshold v_{crit} of the volume fraction, the conducting crystallites form isolated islands and do not contribute to the overall conductivity σ. Above v_{crit} percolation sets in. We thus write σ as a sum of a percolation and a background conductivity[41]

$$\sigma=\frac{(v_c-v_{\text{crit}})^\beta}{1-v_{\text{crit}}}\sigma_c+\frac{1-v_c}{1-v_{\text{crit}}}\sigma_a, \quad v_c\geq v_{\text{crit}}$$
$$\sigma=\sigma_a, \quad v_c<v_{\text{crit}} \tag{6}$$

where σ_a and σ_c are the conductivities of the hot amorphous and the crystalline material, respectively, and β is the percolation exponent (1.5 near $v_c = v_{crit}$ and 1 near $v_c = 1$).[25] Since the main contribution to the temperature dependence again arises from the amorphous material and from the degree of crystallization, we assume a constant value of 3000 $(\Omega\,\text{cm})^{-1}$ for σ_c, neglecting the temperature dependence (the TCR is reported to be positive at room temperature,[2] and negative at elevated temperatures[12]). The critical volume fraction v_{crit} is assumed to decrease linearly with time (from 0.3 at 300 K to 0.1 at 700 K) in order to take the following effects into account: (1) increased conductivity of the amorphous background due to latent heat of crystallization, leading to percolation at volume fractions below the nominal threshold, and (2) modifications of the crystal structure[1,12,28] during the cooldown process.

As a last step we need the temperature dependence of R_a and σ_a of the hot amorphous material. Experimental data is not yet available. The main problem is that static measurements are almost impossible since crystallization can hardly be suppressed when a glassy material is slowly heated or a liquid is slowly cooled. Transient temperature measurements[42] of GeTe will be performed in the future. In this work we used simple linear temperature dependences. The reflectivity R_a of the hot amorphous material is written as

$$R_a = \frac{R_l - 0.4}{T_l - T_g}(T - T_g) + 0.4, \quad T \geq T_g$$
$$R_a = 0.4, \quad T < T_g \tag{7}$$

where T_l is the melting temperature [1000 K (Ref. 1)] and R_l is the reflectivity at T_l. This was determined to be 50% from the saturation value of the height of the melting peak in the transient reflectivity profiles (see Sec. III). T_g is approximated by the crystallization temperature [460 K (Ref. 1)] and the room-temperature amorphous reflectivity at 633 nm is 40%.

Analogously, the conductivity is written as (all temperatures in K)

$$\sigma_a = \frac{\sigma_l}{T_l - T_g}(T - T_g), \quad T \geq T_g$$
$$\sigma_a = 0, \quad T < T_g \tag{8}$$

where σ_l is the conductivity at T_l. Its value was determined to be 630 $(\Omega\,\text{cm})^{-1}$ from the height of the first peak in the transient conductivity profiles at the highest possible fluence (just below ablation). It is an average over the film thickness and smaller than the equilibrium liquid conductivity, as discussed in Sec. III (regime 2).

Inserting Eqs. (7) and (8) into (5) and (6), we find R and σ as functions of temperature and degree of crystallization following laser exposure. Using the time dependences of these variables [Eqs. (2) and (4)] we obtain analytical expressions for R and σ as a function of time. These expressions contain the parameters T_{max} and ν [described after Eqs. (2) and (3), respectively]. Since the threshold fluence for reaching the melting temperature (see above) is between 15 and 20 mJ/cm^2, 1000 K is a reasonable value for T_{max} in fluence regime 3 (intermediate fluence). T_{max} increases with fluence. For the nucleation and growth frequency[19] ν a value of approximately 10^7 s^{-1} (within a factor of 3) is estimated from both the nucleation frequency (Turnbull[39]) and the regrowth velocity (Pamler and Marinero[14]). Although ν is defined at a fixed film temperature T_n [see Eq. (3)], we may expect ν to increase with fluence due to the different thermal history for different fluences.

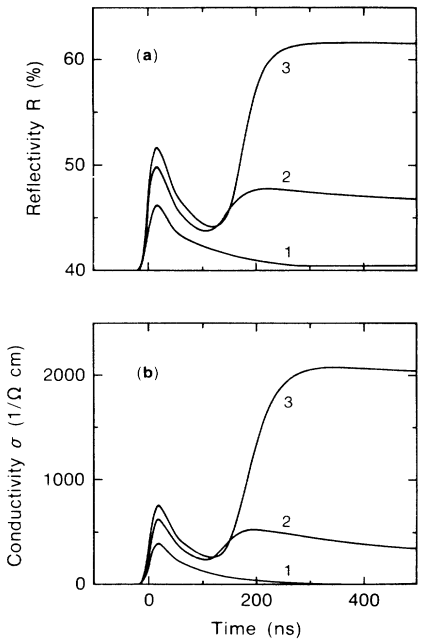

FIG. 9. Computed transient R and σ profiles utilizing the model described in the text and the parameters given in Table I. The curves are numerically smoothed with a resolution of 25 ns.

Calculated time-resolved R and σ profiles using the parameters of Table I are shown in Fig. 9. Comparing these results to the experimental data of Fig. 3, it can be seen that the calculations generate all the characteristic features in the measurements. We note that the values for t_γ, the time interval during the cooldown for which the film temperature is between 600 and 700 K, as determined using Eq. (2), are 40, 95, and 125 ns for curves 1, 2, and 3 of Fig. 9. At a threshold value for t_γ of approximately 50 ns, the second peak (frustrated crystallization) appears in the calculated transient reflectivity profiles. We thus might argue that 600–700 K for at least 50 ns is required to seed nuclei in laser-irradiated GeTe. Further theoretical refinement of the model would allow curve fitting to

TABLE I. Values for the parameters used in the calculation of the transient reflectivity and conductivity profiles shown in Fig. 9.

Fluence regime	Typical fluence (mJ/cm^2)	T_{max} (K)	ν (10^6 s^{-1})	Curve in Fig. 9
2	13	800	5	Curve 1
3	18	1000	5	Curve 2
4	25	1100	6.7	Curve 3

extract accurate numerical values for the parameters. Nevertheless, in spite of the approximations inherent in the model, the qualitative agreement supports the idea of frustrated crystallization in laser-irradiated GeTe films.

V. CONCLUSION

The laser-induced phase transformation from the amorphous to the crystalline state in GeTe has been studied. Utilizing time-resolved optical and electrical probes, we have directly measured for the first time the onset of crystallization during material cooldown. It is determined that a maximum cooling rate must not be exceeded for nucleation and growth to occur. Permanent changes in reflectivity and conductivity mirror the degree of crystallization upon laser irradiation. Conductivity changes are controlled by percolation phenomena (grain interconnection).

The temporal evolution of the optical and electrical changes are successfully modeled by including simple analytical expressions for the time dependence of the film temperature as well as of the temperature dependences of R, σ, and the crystallization rate. The calculations indicate that the film must be maintained at 600–700 K for at least 50 ns in order to induce significant nucleation.

Time resolution of R and σ confirm that partitionless crystallization from the amorphous phase in TeGe films is very rapid (200 ns for complete transformation). Presence of nuclei (seeded by laser exposure) leads to even faster rates as demonstrated in experiments in which a second laser pulse was applied to an area exhibiting frustrated crystallization. In this case, complete transformation of the laser-heated volume was observed within 50 ns and initiated before the sample attained its peak temperature.

ACKNOWLEDGMENTS

It is a pleasure to acknowledge the fruitful discussions with M. O. Thompson (Cornell University), M. Chen, C. J. Lin, K. A. Rubin, J. C. Suits, and C. J. Robinson. Special thanks to Grace Lim for x-ray analysis, to Bill McChesney for preparing the films, and to IBM Corporation for financial support (E.H.).

[1]M. Chen, K. A. Rubin, and R. W. Barton, Appl. Phys. Lett. **49**, 502 (1986).

[2]S. K. Bahl and K. L. Chopra, J. Appl. Phys. **41**, 2196 (1970).

[3]G. B. Fisher and W. E. Spicer, J. Non-Cryst. Solids **8-10**, 978 (1972).

[4]H.-U. Tschirner, I. P. Pazdrij, and R. Weikart, Wiss. Z., Techn. Hochsch. Karl-Marx-Stadt **25**, 219 (1983).

[5]J. C. Valiant and T. E. Faber, Philos. Mag. **29**, 571 (1974).

[6]V. M. Glazov, *Liquid Semiconductors* (Plenum, New York, 1969), p. 289.

[7]W. Schnurnberger, H. Thurn, and H. Krebs, Ber. Bunsenges. Phys. Chem. **80**, 730 (1976).

[8]J. H. Mooij, Phys. Status Solidi A **17**, 521 (1973); P. J. Cote and L. V. Meisel, in *Glassy Metals I,* Vol. 46 of *Topics in Applied Physics,* edited by H.-J. Güntherodt and H. Beck (Springer, Heidelberg, 1982), p. 141.

[9]J. N. Hodgson, Philos. Mag. **8**, 735 (1963).

[10]J. N. Hodgson, Philos. Mag. **6**, 509 (1961).

[11]A. N. Loparev, L. Ya. Min'ko, V. I. Nasonov, and Ya. A. Sukhanov, Zh. Prikl. Spektrosk. **40**, 65 (1984) [J. Appl. Spectrosc. (USSR) **40**, 50 (1984)].

[12]N. Kh. Abrikosov, M. A. Korzhuev, and L. E. Shelimova, Izv. Akad. Nauk SSSR, Neorg. Mater. **13**, 1757 (1977) [Inorg. Mater. (USA) **13**, 1418 (1977)].

[13]E. E. Marinero, W. Pamler, and M. Chen, in *Beam Solid Interactions and Phase Transformations,* edited by H. Kurz, G. L. Olson, and J. M. Poate (Materials Research Society, Pittsburgh, 1986), p. 289.

[14]W. Pamler and E. E. Marinero, J. Appl. Phys. **61**, 2294 (1987).

[15]A. E. Bell, RCA Rev. **40**, 295 (1979).

[16]M. O. Thompson, J. W. Mayer, A. G. Cullis, M. C. Weber, N. G. Chew, J. M. Poate, and D. C. Jacobson, Phys. Rev. Lett. **50**, 896 (1983).

[17]M. O. Thompson and G. J. Galvin, in *Laser-Solid Interactions and Transient Thermal Processing of Materials,* edited by J. Narayan, W. L. Brown, and R. A. Lenons (North-Holland, Amsterdam, 1983), p. 57.

[18]M. Baleva, Phys. Status Solidi B **99**, 341 (1980); P. Nath, S. K. Suri, and K. L. Chopra, Phys. Status Solidi A **30**, 771 (1975); S. K. Bahl and K. L. Chopra, J. Appl. Phys. **40**, 4940 (1969).

[19]We do not explicitly distinguish between nucleation and growth.

[20]This is demonstrated by the fact that when a phase-change material is exposed to a focused laser pulse, the largest crystallites are seen in a circular ring around the center of the beam, and small crystallites inside (too hot) and outside the ring (too cold), C. J. Robinson (private communication); S. Tsukahara, Y. Yokoyama, T. Tanaka, and A. Kokubu, IEEE Trans. Magn. **20**, 1308 (1984).

[21]M. von Allmen and S. S. Lau, in *Laser Annealing of Semiconductors,* edited by J. M. Poate and J. W. Mayer (Academic, New York, 1982), p. 439.

[22]D. Turnbull, Contemp. Phys. **10**, 473 (1969).

[23]K. A. Jackson, in *Surface Modification and Annealing,* edited by J. M. Poate, G. Foti, and D. C. Jacobson (Plenum, New York, 1983), p. 51.

[24]This is derived from realistic heat-flow calculations, J. C. Suits and M. Chen (private communication).

[25]J. M. Ziman, *Models of Disorder* (Cambridge University, Cambridge, England, 1979), pp. 370–379.

[26]Frustrated crystallization (regime 3) is observed for lower fluences (25%) in the case of $Ge_{55}Te_{45}$ (12–18 mJ/cm^2) as compared to GeTe (15–22 mJ/cm^2). This relation may be used to compare results obtained for films of different composition.

[27]See Glazov, Ref. 6, pp. 289–300.

[28]B. Vengalis and K. Valatska, Phys. Status Solidi B **117**, 471 (1983).

[29]P. Baeri and S. U. Campisano, in *Laser Annealing of Semiconductors,* edited by J. M. Poate and J. W. Mayer (Academic, New York, 1982), p. 75.

[30]See Glazov, Ref. 6, p. 200.

[31]*Thermophysical Properties of High Temperature Solid Materials,* edited by Y. S. Touloukian (Macmillan, New York, 1967),

Vol. 6/1, p. 578.

[32]Kh. I. Amirkhanov, Ya. B. Magomedov, and Kh. O. Alieva, Opt.-Mekh. Prom. **52**, 31 (1985) [Sov. J. Opt. Technol. **52**, 408 (1985)].

[33]*Thermophysical Properties of Matter,* edited by Y. S. Touloukian, R. W. Powell, C. Y. Ho, and M. C. Nicolaou (IFI/Plenum, New York, 1973), Vol. 10, p. 577.

[34]H. S. Carslaw and J. C. Jaeger, *Conduction of Heat in Solids* (Clarendon, Oxford, 1959), p. 50–56.

[35]Equation (2) only holds for $t > 20$ ns. For shorter times we limit $T(t)$ to the value T_{max}.

[36]See Carslaw and Jaeger, Ref. 34, pp. 78–80.

[37]Estimated from the devitrification heat of $Ge_{18}Te_{82}$ (12 cal/g) given by P. Clechet, C. Martelet, and Nguyen Dinh Cau, J. Thermal Anal. **16**, 59 (1979), and the heat of fusion (larger than the heat of devitrification) of GeTe (42 cal/g) given by M. A. Korzhuev, L. A. Petrov, O. A. Teplov, and G. K. Demenskiy, Izv. Akad. Nauk SSR Met. **1**, 36 (1983), translated in Russian Metallurgy **1**, 31 (1983).

[38]R. A. Medzhidov and S. M. Rasulov, Teplofiz. Vys. Temp. **14**, 654 (1976) [High Temp. (USSR) **14**, 581 (1976)].

[39]See Turnbull (Ref. 22) and Jackson (Ref. 23).

[40]U. J. Gibson and R. A. Buhrman, Phys. Rev. B **27**, 5046 (1983); G. A. Niklasson and C. G. Granqvist, J. Appl. Phys. **55**, 3382 (1984); Tae Won Noh, Yi Song, Sung-Ik Lee, J. R. Gaines, Hee Dong Park, and Eric R. Kreidler, Phys. Rev. B **33**, 3793 (1986); A. Bittar, S. Berthier, and J. Lafait, J. Phys. (Paris) **45**, 623 (1984).

[41]S. Kirkpatrick, Phys. Rev. Lett. **27**, 1722 (1971).

[42]M. O. Thompson, J. W. Mayer, P. S. Peercy, J. M. Poate, D. C. Jacobson, A. G. Cullis, and N. Chew, Phys. Rev. Lett. **52**, 2360 (1984).

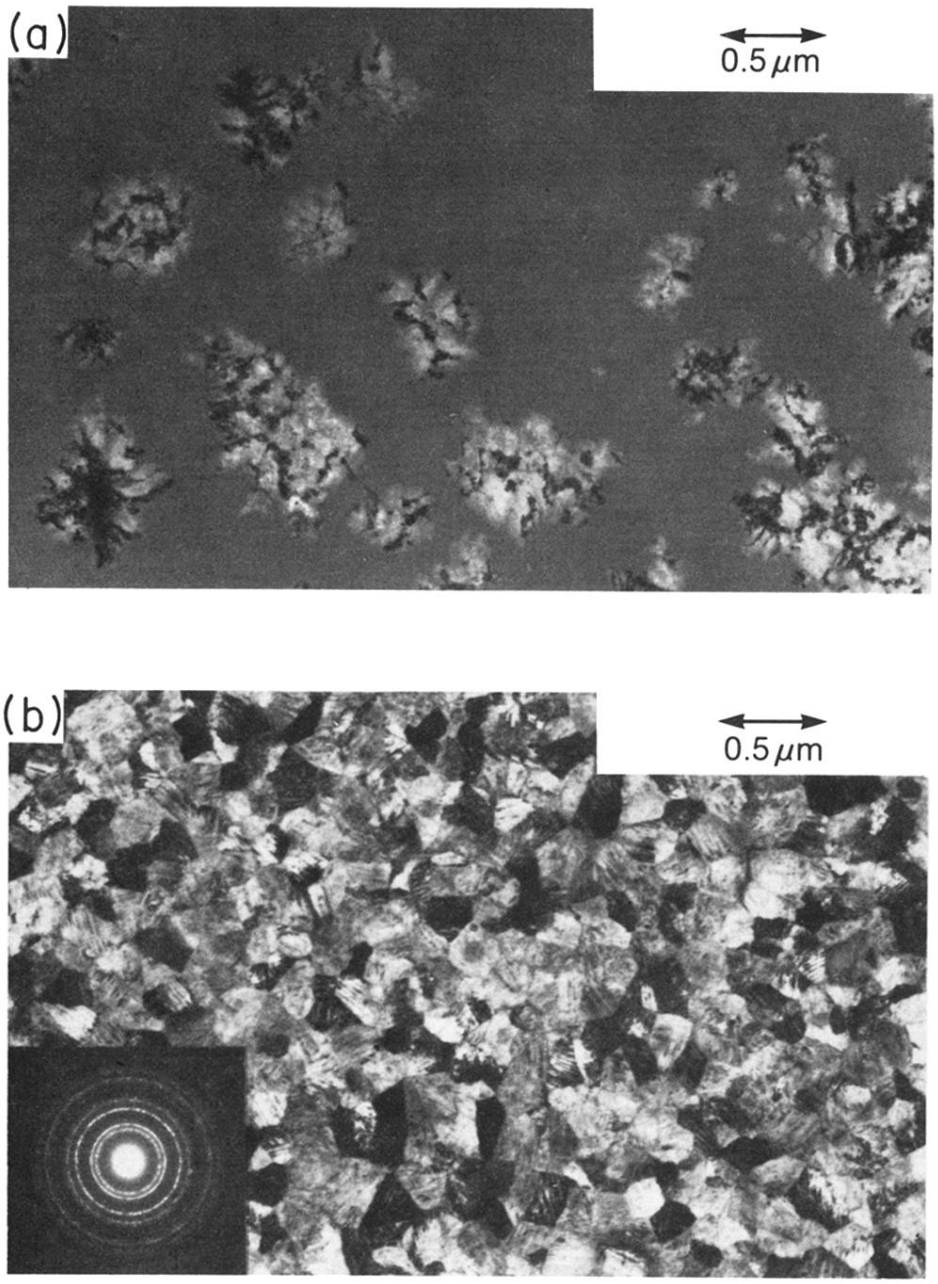

FIG. 6. TEM analysis of $Ge_{55}Te_{45}$ thin films exposed to (a) one and (b) two pulses of 13.5 mJ/cm^2 (see Ref. 26). Significant grain growth is observed in (a) whereas (b) shows complete crystallization of the irradiated area.